

Locked-mode avoidance and recovery with ICRH in Alcator C-Mod

L. Delgado-Aparicio¹, D. A. Gates¹, S. Wolfe², C. Gao², J. E. Rice², T. Golfinopoulos², R. Granetz², S. Wukitch², L. Sugiyama³, M. Greenwald², A. Hubbard², J. Hughes², E. Marmar², P. Phillips⁵, M. L. Reinke², W. Rowan⁵, S. Scott¹ and R. Wilson¹

¹Princeton Plasma Physics Laboratory, Princeton, NJ, 08540, USA

²MIT - Plasma Science and Fusion Center, Cambridge, MA, 02139, USA

³MIT - Laboratory for Nuclear Science, Cambridge, MA, 02139, USA

⁴University of Texas - Austin, TX, 78759, USA

⁵University of York, Heslington, York, YO10 5DD, UK

I) Introduction and motivation.-

Understanding the formation and stability of three-dimensional (3D) helical modes in the core of an otherwise, axisymmetric toroidal configuration, is still one of the challenges of current fusion research [1-5]. Small deviations from toroidal axisymmetry are well known to destabilize non-rotating tearing modes (a.k.a. locked modes), which can significantly impact plasma operation. Error-field induced locked-modes have been studied in several tokamak devices and are observed to result in a density pump-out, braking of core toroidal rotation, modification of sawtooth activity and significant reduction in energy and particle confinement. Locked modes frequently lead to disruptions and associated vertical displacements. Locked-mode excitation can be achieved in C-Mod (see Fig. 1 and ref. [6]) by using the control coils placed outside the vacuum vessel; so far, the locked-mode threshold studies have considered only engineering macroscopic parameters resulting in a scaling law of the form $B_r^{lock}/B_T \propto \bar{n}_e^{\alpha_n} B_T^{\alpha_B} q_{95}^{\alpha_q} R_0^{\alpha_R}$ [6,8]. The determination of this dependence is useful for extrapolating low-aspect and standard-aspect ratio tokamaks results to ITER. However, the influence of drift-MHD as well as collisional and neoclassical flow-damping effects dependent on local kinetic profiles [8-10] can alter the predicted scaling and have not yet been considered. The experimental validation of new theoretical models sensitive to rotation [8] and viscous [11] effects different than that of ideal-MHD should also be addressed.

Locked-mode avoidance in low-density Ohmic discharges is highly desirable, if not crucial, for reliable tokamak operation. The objective of this study is thus two-fold. First, study the evolution of the plasma profiles ($T_{e,i}$ and v_ϕ) during the formation of error-field-induced locked-modes at ITER fields without external sources of fueling and momentum input. And second, attempt “unlocking” the core plasma using available radio frequency techniques such as Ion Cyclotron Resonance Heating (ICRH) and in the future, also, Lower Hybrid Current Drive (LHCD).

II) Locked-modes in C-Mod.-

Error-field-induced locked-modes can be studied in C-Mod at ITER toroidal fields and without

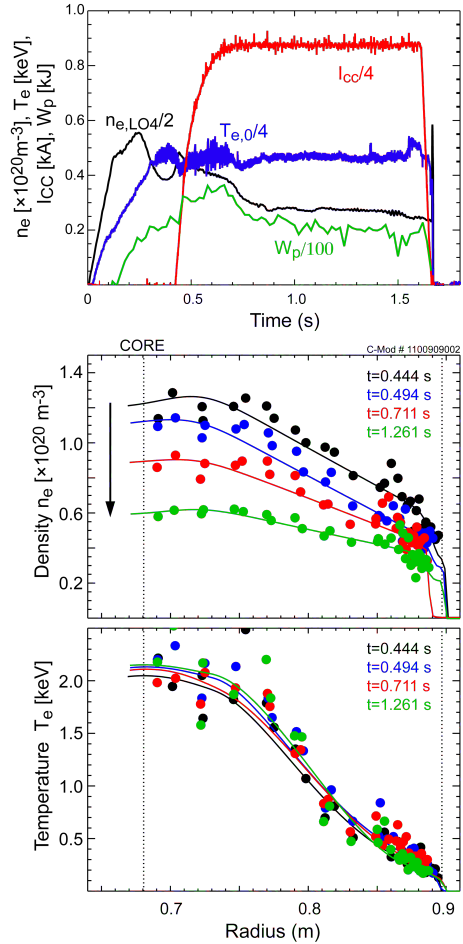


Fig. 1. a) Baseline locked-mode discharge in Alcator C-Mod. n_e and T_e profiles at different times are shown in b) and c).

NBI fueling and momentum input. Locked-modes excitation is achieved in C-Mod by ramping-up a set of external “A-coils” capable of producing non-axisymmetric, predominantly $n=1$, fields with different toroidal phase and a range of poloidal mode m spectra [see [6] and Fig. 1-a)]. The typical plasma discharge parameters were $I_p \sim 0.8$ MA, $B_t \sim 5.4$ T, $T_{e0} \sim 2.0$ keV and $n_{e0} = (0.6-1.4) \times 10^{20} \text{ m}^{-3}$ (see Fig. 1). The safety factor on axis was $q_0 \sim 0.9$ while $q_{95} \sim 4$. As a result, sawteeth activity was present but without long-lived modes [1,2] and fishbones [5].

A strong decrease of the plasma density as shown in Fig. 1-b) is commonly observed in locked-mode discharges. The pump-out at the edge is $\sim 30\%$ while the core density is reduced a factor of two, at nearly constant electron temperature [see Fig. 1-c)]. This density pump-out can cause a reduction in the mode-locking thresholds and is the main cause for the decrease in stored energy, confinement time, β and neutron production. As a result of the density pump-out there is a strong reduction of density fluctuations measured by reflectometer as depicted in Fig. 2-a); the time window between τ_0 and τ_1 corresponds to the raise-time of the control coils to their maximum current of $I_{CC} = 3.5$ kA. The change of the sawtooth instability at $t = \tau_{LM}$ is significant, with temperature excursions in the ramp-up phase changing from $\Delta T_{e,0} \sim 200-250$ eV at a frequency of 200 Hz before the locked mode onset, to $\Delta T_{e,0} \sim 100-150$ eV at 6.6 kHz during the steady state. In addition, strong magnetic signatures in the range of 40-60 kHz (possibly high- m , at the edge) appear during error field penetration and last for the entire locked-mode as shown in Fig. 3. This phenomenon is detected only with magnetic probes and is apparently not core-localized since there is no evidence of such in the SXR, ECE or TCI diagnostic systems. Moreover, the mode amplitude appear large for high- n , which should be falling-off fast with radius.

III) Avoidance and recovery.-

The C-Mod’s ICRH system provides on- and off-axis heating to plasmas where external particle or momentum sources can or should be absent. This capability enables a unique contribution to worldwide research in support of ITER, to study locked-mode thresholds and unlocking by comparing C-Mod results to those from devices that utilize neutral beam injection (NBI). The later can alter the plasma fueling and momentum balance, which is particularly important if the locked-mode threshold including the effects of plasma rotation is such that $(\delta B_{2/1}/B_{t,0})_\omega \approx (\delta B_{2/1}/B_{t,0}) \cdot (0.2\omega_\phi/\omega_D)^{1.5}$, where ω_D is the ion diamagnetic frequency [8]. Along these lines, the use of a high-resolution x-ray crystal imaging spectrometer (CXIS, [12,13]) is highly desirable since its operation does not require using a strong NBI, unlike tangential charge exchange recombination spectrometers (CXRS). Alcator C-Mod x-ray crystal imaging spectrometer is designed to view the entire cross section and can work with intrinsic (Mo) or extrinsic (Ar) impurities in the trace-limit. A snapshot of the time history of the argon core toroidal velocity and ion temperature inferred for

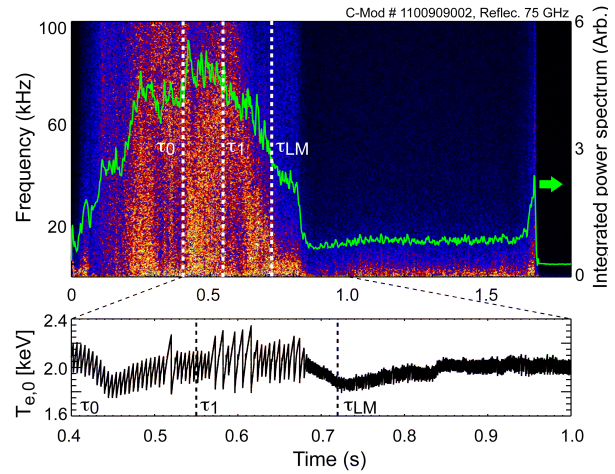


Fig. 2. a) FFT and IPS for density fluctuations. The modification of sawteeth is shown in b).

the raise-time of the control coils to their maximum current of $I_{CC} = 3.5$ kA. The change of the sawtooth instability at $t = \tau_{LM}$ is significant, with temperature excursions in the ramp-up phase changing from $\Delta T_{e,0} \sim 200-250$ eV at a frequency of 200 Hz before the locked mode onset, to $\Delta T_{e,0} \sim 100-150$ eV at 6.6 kHz during the steady state. In addition, strong magnetic signatures in the range of 40-60 kHz (possibly high- m , at the edge) appear during error field penetration and last for the entire locked-mode as shown in Fig. 3. This phenomenon is detected only with magnetic probes and is apparently not core-localized since there is no evidence of such in the SXR, ECE or TCI diagnostic systems. Moreover, the mode amplitude appear large for high- n , which should be falling-off fast with radius.

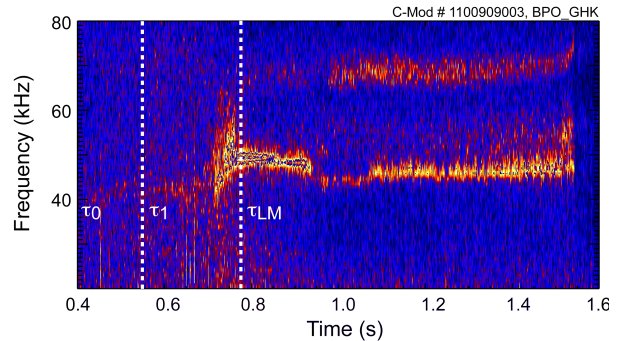


Fig. 3. Spectrogram of magnetic fluctuations during error field penetration and locked-mode.

the raise-time of the control coils to their maximum current of $I_{CC} = 3.5$ kA. The change of the sawtooth instability at $t = \tau_{LM}$ is significant, with temperature excursions in the ramp-up phase changing from $\Delta T_{e,0} \sim 200-250$ eV at a frequency of 200 Hz before the locked mode onset, to $\Delta T_{e,0} \sim 100-150$ eV at 6.6 kHz during the steady state. In addition, strong magnetic signatures in the range of 40-60 kHz (possibly high- m , at the edge) appear during error field penetration and last for the entire locked-mode as shown in Fig. 3. This phenomenon is detected only with magnetic probes and is apparently not core-localized since there is no evidence of such in the SXR, ECE or TCI diagnostic systems. Moreover, the mode amplitude appear large for high- n , which should be falling-off fast with radius.

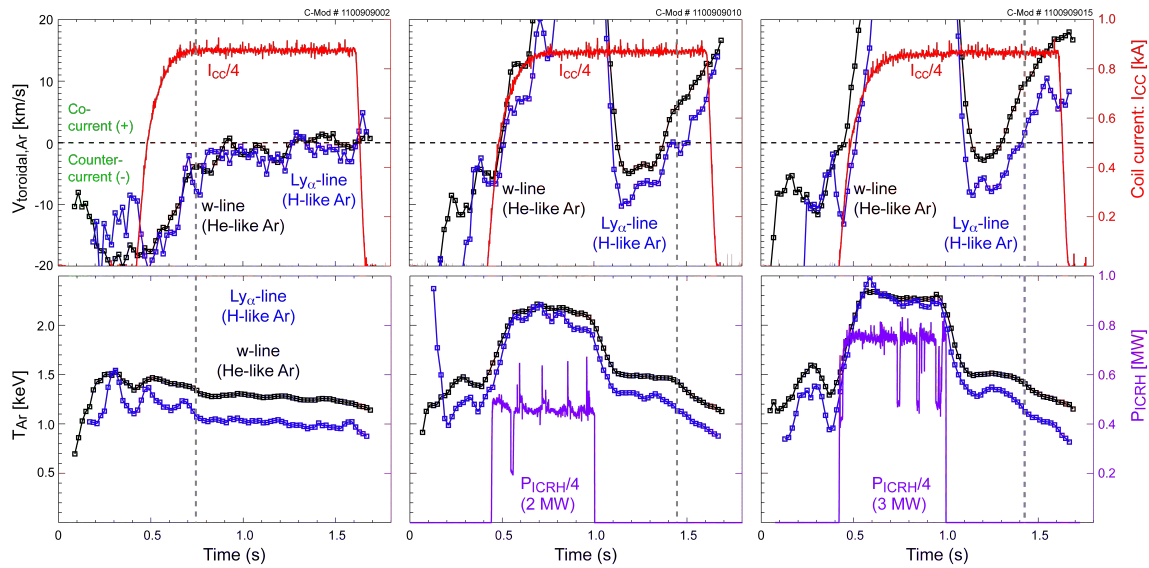


Fig. 4. Time history of the core toroidal velocity and ion temperature inferred for a) the baseline locked-mode discharge and during the use of b) 2 and c) 3 MW of ICRH heating power.

the baseline locked-mode discharge shown in Fig. 1, are depicted in Fig. 4-a). For the toroidal velocity estimates using the Doppler-shift of the He-like-‘w’ and H-like-‘Ly- α ’ lines - shown in Fig. 4, ‘+’ velocity indicates co-current directed rotation, while ‘-’ indicates counter-current. Therefore, the core toroidal velocity during the locked-mode slowed-down from -20 km/s in the counter-current direction to rest, while the ion temperature decreased \sim 200 eV.

a) Early ICRF aim at “delaying” the mode onset (LM avoidance).-

These first experiments considered an ICRH power scan *in-sync* with the I_{CC} ramp-up in the control coils. The use of 1MW (not shown here) delayed the mode-onset but was not sufficient to transition into an H-mode even when the stored energy was doubled from 25 to 55 kJ. However, for $P_{ICRH}=2$ and 3 MW the plasma experienced temporary L \rightarrow H transitions [see Figs. 4-b) and -c)] as the average density, core ion temperature, toroidal velocity and stored energy increased up to $2\times 10^{20} \text{ m}^{-3}$, 2-2.5 keV, 50-60 km/s and 150 kJ, respectively. Nonetheless, when ICRH power is turned off the core plasma “locks” at later times and its characteristic high-frequency magnetic signatures persist. The locking times (τ_{LM}) after the heating pulse are similar for all these cases due to nearly identical time-histories of density, temperature and toroidal flow velocity. This technique may well be used in the future for avoiding plasma disruptions associated with locked-modes. Additional experiments will aim at “fine-tuning” the ICRH power to evaluate the power density threshold for avoiding the mode locking as well as determine whether the H-mode accessibility varies in the presence of error fields.

b) Late ICRF aim at damping/eliminating the mode (LM recovery).-

The second set of experiment considered using ICRF power pulses well into the non-rotating phase in order to change the plasma profiles and its gradients. The locked-mode onset time τ_{LM} (see vertical dotted lines) shown in Figs. 1-3, 4-a) and 5 were reproducible to within ± 65 ms and showed to be sensitive to the density evolution ($\langle n_e \rangle \sim 0.75 \times 10^{20} \text{ m}^{-3}$) in accordance with a strong linear dependence of mode-locking thresholds ($\alpha_n \rightarrow 1$). These L-mode plasmas did not experience transitions to H-mode due to their lower-density ($\sim 1/2$ of the density before locked-mode onset), even though P_{ICRF} was raised from 1 to 3 MW. During the recovery experiments the core electron and ion temperature increase only 400, 600, 1000 eV when heated with $P_{ICRF}=1, 2$ and 3 MW, respectively (see Fig. 5). The density augments were small and the stored energy increased 20, 35, 55 kJ, respectively. The high-frequency magnetic signatures remain when 1MW was applied but were successfully suppressed for the cases with $P_{ICRF}=2$ and 3 MW

(not shown here). One interesting detail is that the change in toroidal rotation (see Fig. 5) *points* in the counter-current direction recovering the direction and magnitude of the toroidal flow before the formation of the locked-mode, but contrary to the expected Rice-scaling in the co-current direction [14]. However, the locked mode occurs at a low density near the LOC/SOC transition where rotation reversals are commonly observed [15]. It is thought that P_{ICRH} is changing the temperature and density gradients at the edge, that generate a toroidal flow through anomalous momentum transport, which in turn “unlocks” the core plasma. As mentioned above, the toroidal velocity is a very attractive parameter for scaling the locked-mode thresholds by its direct relation with the viscous torque. As an example, the temperature gradient changed from $\nabla T_e \sim 16$ keV/m in the Ohmic phase to $\nabla T_e \sim 23$ keV/m when 3 MW of ICRH power was applied. In the future, the changes of ion temperatures and flows at the edge should be assed using CXRS.

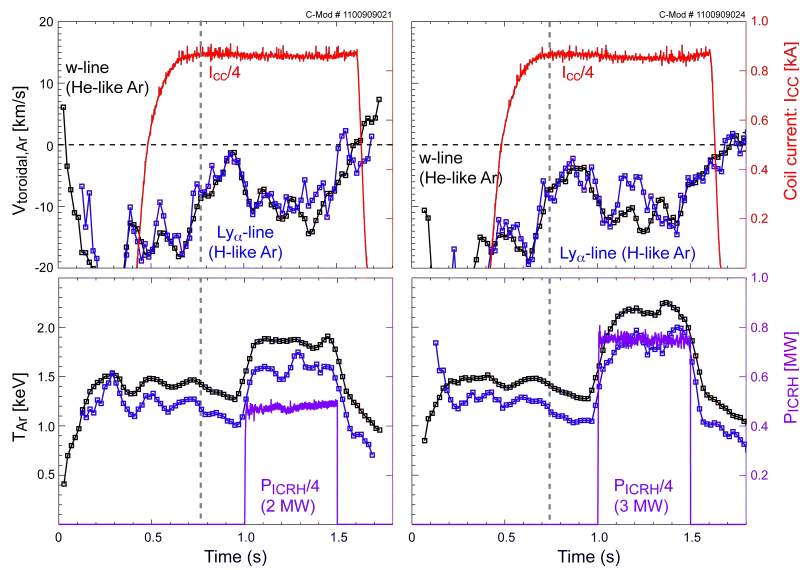


Fig. 5. Time history of the $V_{t,0}$ and $T_{i,0}$ inferred for the a) 2 MW and b) 3 MW ICRH heated locked-mode discharges.

In summary, locked-modes can be studied in C-Mod at ITER-B_t, without NBI fueling and momentum input. Delay of the mode-onset and locked mode recovery have been successfully obtained in C-Mod without external momentum input using ICRH. The use of external heating *in-sync* with the error-field ramp-up resulted in a successful delayed of the mode-onset when $P_{ICRH} \geq 1$ MW, which demonstrate the existence of a power threshold to “unlock” the mode; in the presence of an error field the L-mode discharge can transition into H-mode only when $P_{ICRH} \geq 2$ MW and at high densities. During the recovery experiments the “induced” toroidal rotation was in the counter-current direction recuperating the direction and magnitude of the toroidal flow before the mode onset. However, once P_{ICRH} is turned off, the core plasma “locks” at later times depending on the evolution of n_e and V_t . Studying the connection between $\nabla T_{e,i}$ and V_t through the residual stress and the effects of neoclassical toroidal viscosity (NTV) and toroidal rotation will shed light on the mechanisms unlocking the core plasma. This work was performed under US DoE contracts including DE-FC02-99ER54512 and others at MIT and DE-AC02-09CH11466 at PPPL.

- [1] L. Delgado-Aparicio, *et al.*, Phys. Rev. Letters, **110**, 065006, (2013).
- [2] L. Delgado-Aparicio, *et al.*, Nucl. Fusion, **53**, 043019, (2013).
- [3] J. Menard, *et al.*, Phys. Rev. Letters, **97**, 095002, (2006).
- [4] I. T. Chapman, *et al.*, Nucl. Fusion, **50**, 045007, (2010).
- [5] L. Delgado-Aparicio, *et al.*, to be submitted to Phys. Plasmas, (2014).
- [6] S. M. Wolfe, *et al.*, PoP, **12**, 056110, (2005).
- [7] J. E. Menard, *et al.*, Nucl. Fusion, **50**, 045008, (2010).
- [8] J-K. Park, *et al.*, Nucl. Fusion, **52**, 023004, (2012).
- [9] A. Cole, *et al.*, Phys. Plasmas, **13**, 032503, (2006).
- [10] A. B. Mikhailovskii, *et al.*, Plasma Phys. Rep., **21**, 789, (1995).
- [11] A. Cole, *et al.*, Phys. Rev. Letters, **99**, 065001, (2007).
- [12] M. L. Reinke, *et al.*, Rev. Sci. Instrum., **83**, 113504, (2012).
- [13] L. Delgado-Aparicio, *et al.*, Plasma Phys. Control. Fusion, **55**, 125011, (2013).
- [14] J. E. Rice, *et al.*, Nucl. Fusion **47**, 1618, (2007).
- [15] J. E. Rice, *et al.*, Phys. Plasmas, **19**, 056106 (2012).